

Experimental crystallization of chevkinite/perrierite from *REE*-enriched silicate liquids at high pressure and temperature

T. H. GREEN AND N. J. PEARSON

School of Earth Sciences, Macquarie University, North Ryde, NSW 2113, Australia

Abstract

Chevkinite/perrierite crystallized from a series of *REE*-enriched compositions, ranging from basalt through andesite to rhyolite at pressures from 7.5 to 20 kbar and temperatures from 900–1050 °C. The Al_2O_3 content increased with increasing pressure, but no other consistent composition change was observed with pressure and temperature variation in this range. The *REE* partition pattern consistently favoured light over heavy *REE*, with a regular decrease in partition coefficients (*D*) from La through to Lu. *D* values increase with decreasing temperature and decreasing *REE* content (i.e. Henry's Law does not apply, as *REE* are essential structural constituents of chevkinite/perrierite), but appear unaffected by pressure and f_{O_2} . Chevkinite/perrierite may be a significant fractionating phase in evolving silicic magmas, or a residual phase from low degrees of partial melting of granulites. In both these circumstances it will exert a major control on the *REE* content of derivative liquids.

KEYWORDS: chevkinite, perrierite, rare earth elements, silicate liquids.

Introduction

THE Ti, rare earth element (*REE*)-rich accessory phase chevkinite/perrierite has been recently recorded from silicic members of several different igneous rock suites (e.g. Jaffe *et al.*, 1956; Izett and Wilcox, 1968; McDowell, 1979; Ewart, 1981; Harding *et al.*, 1982; Haggerty and Mariano, 1983; van Bergen, 1984) and from granulites from Antarctica (De Paolo *et al.*, 1982). Optically it is difficult to distinguish chevkinite/perrierite from rutile and/or allanite, and it is anticipated that with further detailed mineralogical studies using the microprobe, there will be many more reports of its occurrence. As discussed later, it is not possible to distinguish chevkinite from perrierite on the basis of compositional data alone. Hence for the purpose of this paper the term chevkinite/perrierite is used, since X-ray data could not be obtained on the small, rare crystals of the phase obtained in experimental runs.

The *REE* and other trace elements (e.g. Zr, Nb, Ta, Y, Th) are readily accommodated in the chevkinite/perrierite lattice, and thus it will have an extremely important role in controlling the abundance of these elements in any evolving magma from which it crystallizes. Hence detailed

knowledge of the geochemistry of chevkinite/perrierite and the pattern of trace element partitioning between this phase and coexisting silicate liquid will be essential for closely controlled modelling of crystal fractionation processes incorporating chevkinite/perrierite.

The present work reports on the composition of chevkinite/perrierite crystallized from a range of *REE*-enriched compositions prepared as part of a wider study of the geochemistry and role of Ti-rich phases in the evolution of magmas (Green and Pearson, 1986*a, b*). The synthetic chevkinite/perrierite compositions obtained for a pressure (*P*), temperature (*T*) range from 7.5–20 kbar and 900–1050 °C are compared with natural examples, and the *REE* partitioning pattern is documented. However, because the *REE* behave as essential structural constituents (ESC) (Sun and Hanson, 1975) in chevkinite/perrierite, the magnitude of the partition coefficients is not relevant to natural rocks, because of high, artificial enrichment of the *REE* in the starting compositions used in this work. Nevertheless the *pattern* of element partitioning is significant, and may be applied to natural systems.

Thus the present study sets out to establish conditions where chevkinite/perrierite may crystallize from magmas, to determine any compositional

changes in chevkinite/perrierite with P, T and to record experimentally determined patterns of element partitioning for the *REE*.

Experimental and analytical procedures

Two series of starting compositions were prepared and these are presented in Table 1. The first series consisted of basalt, basaltic andesite, andesite and rhyodacite to which sphene components and a *REE*-enriched glass were added, as part of a study of sphene saturation and *REE* partitioning between sphene and coexisting silicate liquid (Green and Pearson, 1986a, b). Powdered natural rocks were mixed with various proportions of sphene components and 10% *REE*-enriched glass, melted together, and then quenched to a glass (twice, with fine grinding in between).

The second series of compositions consisted of natural chevkinite or allanite-bearing rhyolites from Queensland (Ewart, 1981), and a Fijian andesite (Gill, 1970), to which *REE*-enriched glass and chevkinite or allanite were added (see Table 1 for details), mixed, melted and quenched to a glass (twice, with fine grinding in between). The aim of experiments on these compositions, prepared specifically for this study, was to synthesize chevkinite from compositions where it was known to occur naturally (in the case of rhyolites), in order to compare natural and synthetic compositions, and to determine possible compositional factors controlling the crystallization of chevkinite/perrierite from common magmas. The chevkinite or allanite-enriched andesites were prepared for the latter purpose. Different amounts of *REE* glass were added to the two rhyolite compositions to allow evaluation of the effect of *REE* content on crystallization of chevkinite and *REE* partitioning between chevkinite and silicate liquid.

The synthetic sphene, chevkinite and allanite com-

ponents were made up from analytical reagent grade chemicals (major element oxides) or from SPEC pure oxides (trace elements—*REE*, Sr, Zr, Nb).

About 5–6 mg of powdered glass, and 2, 5 or 10% wt. of water, measured in with a microsyringe, were encapsulated in silver-palladium ($Ag_{70}Pd_{30}$) tubes and run in multi-capsule pressure cells in a piston-cylinder apparatus, using cell components and techniques documented elsewhere (Green and Pearson, 1985). Nominal pressures using a piston-in procedure were corrected by -10% (Green *et al.*, 1966). Temperatures were measured with a Pt/Pt 10% Rh thermocouple, uncorrected for any effect of pressure on the e.m.f. Temperatures are believed accurate to $\pm 15^\circ C$, allowing for $\pm 5^\circ C$ variation about the set point and $\pm 10^\circ C$ uncertainty due to temperature gradient within the graphite furnace. Run times for these synthesis experiments varied from 24 hours at $900^\circ C$ to 4 hours at $1100^\circ C$. The oxygen fugacity (f_{O_2}) of these standard runs approximates the magnetite-wüstite (MW) buffer (Green and Pearson, 1985), but additional experiments were carried out using a double-capsule technique, with the Ag-Pd sample capsule packed in haematite-magnetite (HM) and sealed in an outer gold capsule. Times for these runs were restricted to $1\frac{1}{2}$ hours in order to ensure preservation of the HM buffer. This was confirmed optically at the end of the experiment. At the conclusion of all runs, the sample was crushed, examined optically and then fragments mounted in resin and polished for electron microprobe analysis.

An ETEC autoprobe was used for the microprobe analysis, with operating conditions and procedures similar to those outlined in Watson and Green (1981) and Green and Pearson (1985). Where possible, a large number of analyses of each phase was obtained and averages determined, because of the relatively low count rates for the *REE* at the 15 kV accelerating voltage used. This was chosen as a compromise, to allow analysis of

Table 1. Natural rock compositions used in the experimental work, together with composition of the additives to the natural rocks. 10wt.% of the *REE* glass together with 10, 10, 7.5 and 5wt.% sphene components were added to the basalt, basaltic andesite, andesite and rhyodacite, respectively. 5wt.% of *REE* glass together with 5wt.% allanite were added to the Binna Burra rhyolite, while 10wt.% *REE* glass and 5wt.% chevkinite were added to the Mt. Gillies rhyolite. 5wt.% *REE* glass and either 10wt.% chevkinite or 10wt.% allanite were added to the andesite (i.e. second and third modified andesite compositions, respectively).

	basalt	basaltic andesite	andesite	rhyodacite	REE glass*	sphene	rhyolite (Mt. Gillies)	rhyolite (Binna Burra)	chevkinite**	allanite***
SiO ₂	48.10	54.09	61.19	73.55	50	28.60	76.06	77.12	19.5	30.0
TiO ₂	1.70	0.56	0.68	0.27	—	38.03	0.15	0.06	19.5	2.4
Al ₂ O ₃	16.00	17.76	17.10	14.31	12	—	12.13	12.60	—	12.2
Fe _{TOT}	8.60	9.82	5.37	1.79	—	3.67	1.51	0.93	10.0	17.01
MnO	0.10	0.19	0.13	0.04	—	—	0.03	0.01	—	—
MgO	10.60	4.02	2.98	0.58	—	—	0.17	0.03	—	—
CaO	11.10	11.14	7.28	1.57	5	26.70	0.71	0.62	4.0	9.9
Na ₂ O	2.50	1.78	3.67	3.25	4	—	3.17	2.91	—	—
K ₂ O	1.60	0.56	1.39	4.49	4	—	6.00	5.71	—	—
F ₂ O ₅	—	0.08	0.21	0.15	—	—	—	—	—	—
F	—	—	—	—	—	3.37	—	—	0.4	0.3

* additional oxides present as 5wt. each of SrO, La₂O₃, Sm₂O₃, Ho₂O₃ and Lu₂O₃

** additional oxides present are (in wt.%) 0.8 ZrO₂, 0.8 Nb₂O₅, 14.0 La₂O₃, 22.0 Ce₂O₃, 8.0 Nd₂O₃, 0.3 Sm₂O₃, 0.5 Ho₂O₃, 0.2 Lu₂O₃.

*** additional oxides present are (in wt.%) 8.0 La₂O₃, 12.1 Ce₂O₃, 5.0 Nd₂O₃, 0.4 Sm₂O₃, 0.6 Ho₂O₃, 0.2 Lu₂O₃.

other major elements at the same time as the REE, and to allow the smallest possible crystals, or glass areas, to be analysed without interference from neighbouring phases.

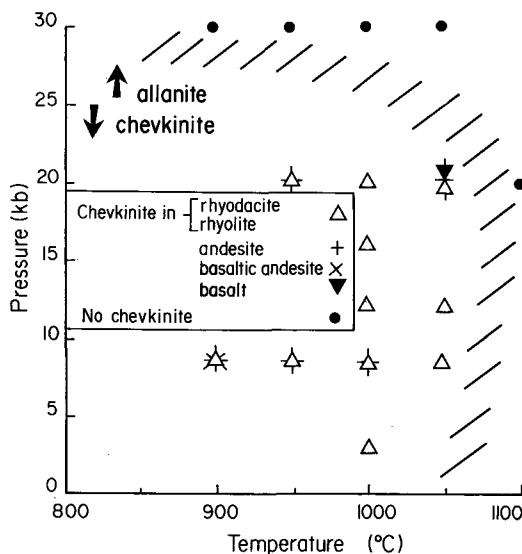


FIG. 1. Pressure-temperature diagram showing conditions at which chevkinite/perrierite crystallized from a range of REE-enriched compositions. Shaded area denotes P, T conditions above which chevkinite/perrierite was not obtained. Instead, as denoted by the upward pointing arrow, allanite crystallized from these REE-enriched compositions. The downward pointing arrow denotes the P, T field where chevkinite/perrierite crystallized.

Results

Stability. Chevkinite/perrierite was synthesized from REE, sphene-enriched natural compositions (ranging from basalt to rhyodacite) or from chevkinite or allanite-enriched andesite and rhyolite at pressures of 2.5–20 kbar and temperatures of 900–1050°C (Fig. 1). The lower temperature of stability was not defined experimentally, though McDowell (1979) proposed that chevkinite formed from a granitic magma at 700–750°C, and it is stable at sub-solidus conditions (e.g. it is recorded from granulite facies rocks—De Paolo *et al.*, 1982). Chevkinite/perrierite did not crystallize at 1100°C or at 30 kbar from the above compositions, although it formed at 30 kbar, 1050°C from a synthetic REE-rich sphene composition (along with REE-rich sphene and rutile).

Composition features. Representative analyses of chevkinite/perrierites are given in Table 2, and all analyses are plotted in Figs. 2 and 3. Adopting a

general formula $A_4^{IX}B^{VI}C_4^{VI}O_8(Si_2O_7)_2$, element substitution follows a coupling: $Ca_A^{2+} + Sr_A^{2+} + Ti_C^{4+} \rightleftharpoons REE_A^{3+} + M_{B,C}$ where $M = Fe, Al, Mg, Zr, Nb, P, K$ as shown by Fig. 2. It should be noted that in this figure divalent Fe in the B site has been included in the ordinate parameter so that the array of points falls close to an ideal 4:5 relationship, consistent with the general formula given earlier. Fig. 2 also shows that a wider range of chevkinite/perrierite compositions was obtained experimentally than has so far been recorded in natural examples.

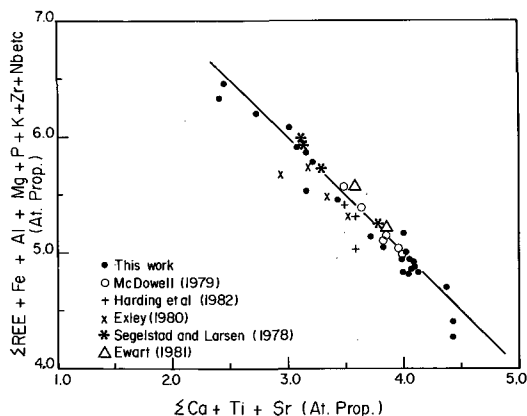


FIG. 2. Composition plot of elements (atomic proportions) in the A, B and C sites of synthetic chevkinite/perrierite, compared with natural examples selected from the literature. Two points with a tie-bar represent separate distinct composition populations observed in one run.

Fig. 3 attempts to distinguish between chevkinite and perrierite, and has been plotted following Segalstad and Larsen (1978), using their boundaries for separation of the two minerals, for both synthetic and natural examples. This figure shows that the compositions obtained in this study straddle the boundary between the chevkinite and perrierite fields, irrespective of whether the boundaries between natural or synthetic chevkinites and perrierites are considered. In fact, as noted by Haggerty and Mariano (1983), it is extremely difficult to unequivocally separate chevkinite and perrierite on the basis of composition and average ionic radius of elements occupying particular sites. Hence, in the absence of X-ray powder data and unit cell constants determined therefrom, the phases obtained in this work are best termed chevkinite/perrierite, without attempting the separation as depicted in Fig. 3. Nevertheless, this figure usefully shows that there are two clear compositional groupings;

Table 2. Representative electron microprobe analyses of chevkinite/perrierite from a variety of compositions and different physical conditions. The totals are consistently low, as has been noted in other microprobe analyses of chevkinite (McDowell, 1979; Harding et al., 1982; van Bergen, 1984). This may be due to difficulties in using the Drake and Weill (1972) REE glasses as standards for phases with high REE content, coupled with possible problems with the standard matrix correction procedure when applied to REE-rich phases, and "edge" effects in electron microprobe analyses of crystals with size <10 μ . Abbreviations: comp = composition, RD = rhyodacite, RG+ch = Mt Gillies rhyolite + chevkinite, A + ch = andesite + chevkinite, B = basalt, BA = basaltic andesite. HM = haematite-magnetite buffer. P = pressure, T = temperature, H₂O denotes wt.% water added, n = number of analyses cp = clinopyroxene, all = allanite, sph = sphene, qtz = quartz, amph = amphibole, ilm = ilmenite, ga = garnet, ru = rutile, plag = plagioclase, mag = magnetite, n.d. = below detection limit, - denotes oxide not added to mix and not analysed for.

Run No.	914	911	947	948	948	940	936	953 HM
Comp.	RD	RD	RG+ch	RG+ch	A+ch	B	BA	BA
P(kb)	16	20	20	20	20	20	7.5	7.5
T(°C)	1000	950	950	1050	1050	1050	900	900
t(hrs)	7.5	12	12	6	6	6	24	3
H ₂ O (wt.%)	5	10	10	5	5	5	5	5
n	2	9	15	15	15	1	12	11
Phases	sph	sph,all(?)	qtz	-	cpx,all	cpx,amph, ilm,ga,ru, sph	cpx,plag, sph	amph,cpx, sph,mag
SiO ₂	21.10	19.29	18.36	18.78	21.14	21.99	19.47	18.74
TiO ₂	18.21	18.59	15.36	15.40	19.55	20.81	18.06	16.89
Al ₂ O ₃	5.35	4.95	4.25	4.53	5.81	6.54	3.59	2.42
FeO	2.41	2.78	4.98	4.67	2.91	2.66	3.81	5.78
MgO	0.68	0.67	0.15	0.15	1.06	0.99	0.75	0.87
CaO	5.39	4.93	2.39	2.50	6.09	6.48	5.87	6.14
K ₂ O	0.16	0.13	0.07	0.10	0.05	0.20	0.05	n.d.
P ₂ O ₅	0.35	0.34	n.d.	n.d.	0.25	n.d.	0.27	0.47
SrO	0.65	0.66	0.61	0.62	0.25	1.78	0.27	0.32
La ₂ O ₃	19.90	20.42	15.08	14.54	11.44	24.44	22.18	23.44
Ce ₂ O ₃	-	-	13.46	13.91	15.85	-	-	-
Nd ₂ O ₃	-	-	5.07	5.15	6.48	-	-	-
Sm ₂ O ₃	11.84	12.17	5.98	6.22	2.43	9.48	11.07	7.78
Ho ₂ O ₃	5.68	5.64	4.25	4.10	1.63	1.50	5.17	4.22
Lu ₂ O ₃	5.35	5.01	4.95	4.51	1.20	0.83	5.99	5.88
ZrO ₂	-	-	n.d.	n.d.	0.31	-	-	-
Nb ₂ O ₅	-	-	0.26	n.d.	0.18	-	-	-
	97.07	95.58	95.40	95.56	96.63	97.70	96.55	92.95
Cations based on 22 oxygens								
Si	3.943	4.169	4.001	4.050	4.052	4.094	4.004	4.014
Ti	2.858	2.706	2.517	2.497	2.818	2.914	2.793	2.720
Al	1.192	1.246	1.091	1.151	1.312	1.435	.870	.611
Fe	.475	.398	.908	.842	.466	.414	.655	1.035
Mg	.204	.200	.049	.048	.303	.275	.230	.278
Ca	1.080	1.141	.558	.578	1.251	1.293	1.293	1.409
K	.034	.040	.019	.028	.012	.048	.013	-
P	.059	.059	-	-	.041	-	.047	.085
Sr	.078	.074	.077	.078	.028	.192	.032	.040
La	1.539	1.450	1.212	1.156	.809	1.678	1.682	1.851
Ce	-	-	1.074	1.098	1.112	-	-	-
Nd	-	-	.395	.397	.444	-	-	-
Sm	.857	.806	.449	.462	.160	.608	.784	.574
Ho	.367	.357	.294	.281	.099	.089	.338	.287
Lu	.309	.319	.326	.294	.069	.047	.372	.380
Zr	-	-	-	-	.029	-	-	-
Nb	-	-	.026	-	.016	-	-	-
	12.995	12.967	13.014	12.998	13.020	13.087	13.115	13.285

(a) the chevkinite/perrierite from the chevkinite- or allanite-enriched andesite and rhyolite compositions (containing a higher proportion of light REE), together with the chevkinite/perrierite from the sphene-enriched basalt, show a high average A-site

ionic radius; (b) the chevkinite/perrierites from the remaining sphene-enriched compositions show a distinctly lower average ionic radius for the A-site.

The foregoing observations on the compositional variations noted for chevkinite/perrierite suggest

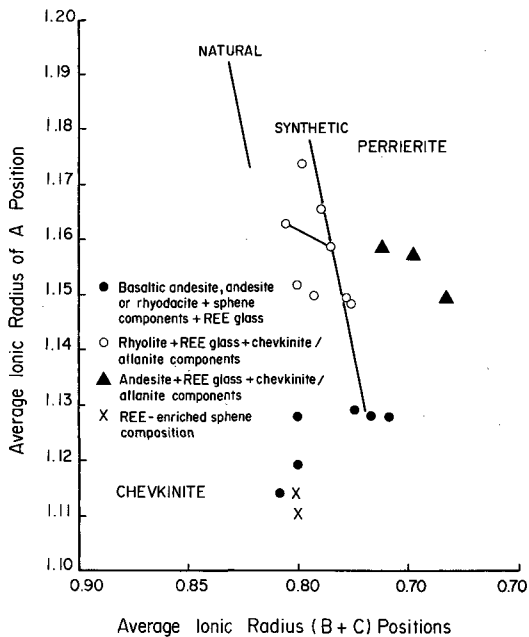
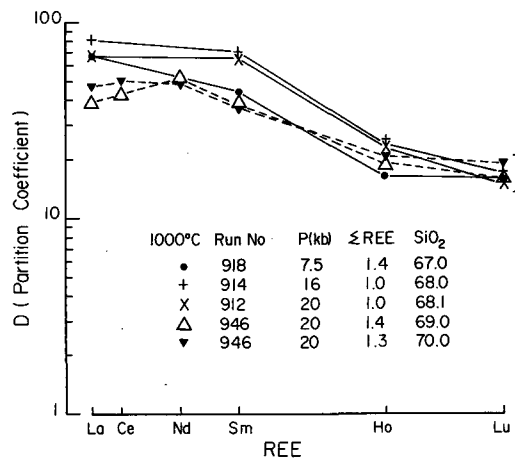
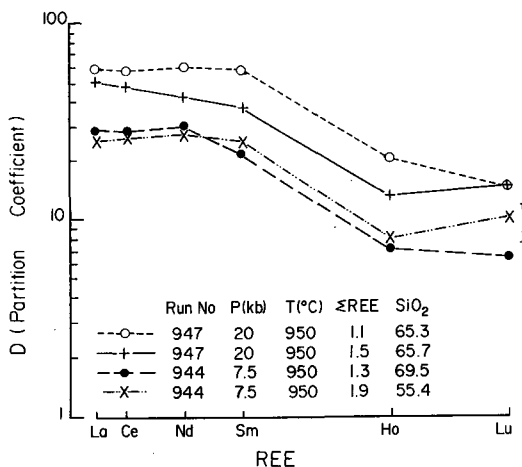


FIG. 3. Average ionic radi of (B+C) positions versus average ionic radius of the A position, following the scheme of Segelstad and Larsen (1978). Ionic radii from Shannon and Prewitt (1969) were used.

that the A-site compositional variation is a function of the bulk composition, rather than a function of the pressure and temperature variation, at least in the 7.5–20 kbar and 900–1050 °C range. However the chevkinite/perrierite from the same starting composition (e.g. rhyodacite) does show increasing Al_2O_3 with increasing P at 1000 °C (e.g. 3.1 wt. % Al_2O_3 at 7.5 kbar to 5.4 wt. % Al_2O_3 at 16 kbar to 6.3 wt. % Al_2O_3 at 20 kbar). Chevkinite/perrierite formed at 7.5 kbar, 900 °C from basaltic andesite at HM and \sim MW buffered conditions shows an increase in Fe with increasing f_{O_2} , and a decrease in Al_2O_3 , reflecting an anticipated increased Fe^{3+} content with increasing f_{O_2} .

REE partitioning. Selected REE partitioning data (D values) from a total of 19 coexisting chevkinite/perrierite and silicate liquid pairs are given in Figs. 4–7. These figures show consistent patterns of LREE enrichment, with a flat to gentle slope for La to Sm, then with a sharp fall between Sm and Ho to a rather flat pattern for the HREE, Ho to Lu. However, even the HREE are far more readily accommodated in chevkinite/perrierite than in the silicate liquid. Since the LREE clearly are ESC in the chevkinite/perrierite lattice, Henry's Law does not apply (e.g. Hanson and Langmuir, 1978), and the D values will vary with REE concentration in

the liquid, increasing with decreasing REE content. This is illustrated for the LREE by comparing the 2 sets of D values for run 947 in Fig. 4 and for runs 912 and 946 in Fig. 5, where P , T and bulk composition are constant, but the ΣREE content varies. In these runs D values for La–Sm are significantly



FIGS. 4 and 5. FIG. 4 (top). Partitioning of REE between chevkinite/perrierite and coexisting basaltic andesitic or rhyodacitic liquids. The data sets at 20 kbar, 950 °C show the effect of variable REE content on D , while the data of 7.5 kbar, compared with the 20 kbar data, show the combined effect of bulk composition and pressure on D values. Error bars in Figs. 4–7 represent uncertainty in D values based on replicate analyses (cf. Green and Pearson, 1985). Also, ΣREE , SiO_2 refer to total weight percent of RE oxides and SiO_2 , respectively, in the glass compositions. FIG. 5 (bottom). Partitioning of REE between chevkinite/perrierite and coexisting rhyodacitic to rhyolitic liquids with variable pressure (for 4 added REE) (runs 918, 914, 912) and for constant pressure but 4 or 6 added REE (runs 912, 946).

different, but are similar for Lu. It is possible that the more incompatible *HREE* do not behave as ESC in the chevkinite/perrierite structure, and so their *D* values are not dependent on *REE* concentration.

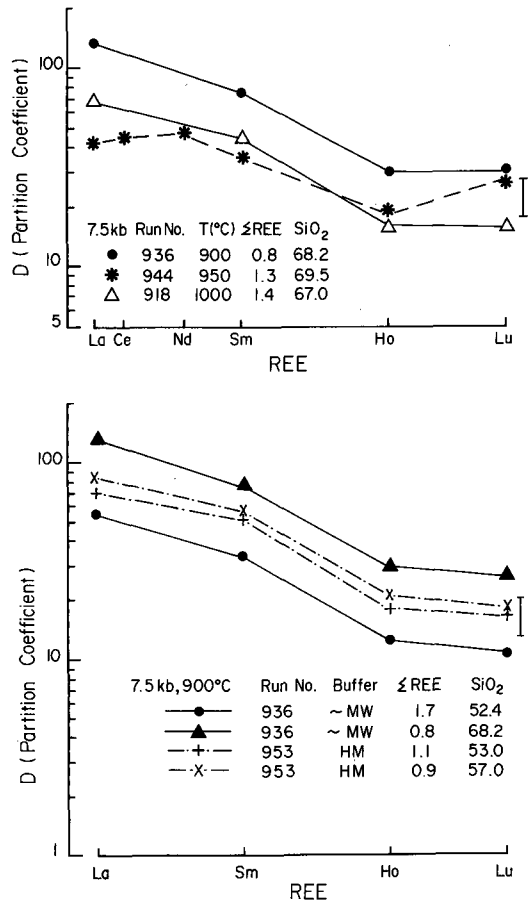
Thus the absolute *D* values for the *LREE* reported in this study cannot be applied directly to natural systems, where the *REE* content is typically one or two orders of magnitude lower. Nevertheless, the *shape* of the *REE D* pattern is relevant, and gives a closer control on modelled *REE* behaviour when chevkinite/perrierite is a fractionating phase, since this work represents the first documented total *D* pattern for the *REE*. Values of 878–1281 for $D_{\text{Ce}}^{\text{chev/liq}}$ from a rhyolite (Ewart, 1982) and of 880 and 1057 for $D_{\text{La}}^{\text{chev/liq}}$ and $D_{\text{Ce}}^{\text{chev/liq}}$ respectively from a rhyodacite (van Bergen, 1984) suggest that the experimentally determined *D* values may be about an order of magnitude lower than expected in natural systems, at similar temperatures, and for similar bulk composition (in terms of major elements) to those used in the present work (e.g. compared with $D_{\text{La}}^{\text{chev/liq}}$ of 131 for rhyolite at 900 °C).

Figs. 5 and 6 illustrate a *REE* compositional control on the *D* pattern, since the patterns for the compositions in which Ce and Nd were added (in addition to La, Sm, Ho and Lu added to all compositions) consistently show lower *D* values for the *LREE* (even when total *REE* content is similar) and similar values for the *HREE* when compared with *D* values obtained for the compositions with only La, Sm, Ho, Lu (e.g. compare runs 944, 918).

Major element composition (in particular, SiO_2 content) and temperature appear to affect the *D* values, with higher *D* for lower *T* (see Fig. 6, runs 918, 936) and more silicic compositions (see Figs. 4 and 7). However, in both these cases some of the difference in *D* values may be contributed to by differences in *REE* content, and it is not possible to clearly separate effects of *REE* content on the one hand, and *T* and major element composition on the other.

D values obtained at different pressures (Fig. 5) do not show a consistent variation with changing *P*, at least in the 7.5–20 kbar range. Finally, *D* values appear unchanged as f_{O_2} is increased from ~ MW buffer to the HM buffer (Fig. 7), since any differences between results for runs 953 (HM buffer) and 936 (~ MW buffer), both at 7.5 kbar, 900 °C, may be attributed to the already established effects of variable bulk composition and *REE* content.

Partitioning data for Sr, as an analogue for Eu^{2+} , have not been plotted in Figs. 4–7 because of the uniformly low *D* values (ranging from 0.4 to 1.4) and absence of any consistent variation with compositional or physical parameters.



FIGS. 6 and 7. FIG. 6 (top). Partitioning of *REE* between chevkinite/perrierite and silicate liquid as a function of temperature. FIG. 7 (bottom). Partitioning of *REE* between chevkinite/perrierite and silicate liquid for variable oxygen fugacity (f_{O_2} ~ MW buffer, or HM buffer).

Discussion

Compositional variation. As indicated in Fig. 2 chevkinite/perrierite may show considerable compositional variation, essentially following the coupled substitution $\text{Ca}^{2+} + \text{Sr}^{2+} + \text{Ti}^{4+} \rightleftharpoons \text{REE}^{3+} + \text{M}^{3+,2+}$. In the experimental work, this substitution appears to be controlled by the bulk composition. This is consistent with the wide range of chevkinite/perrierite compositions crystallizing from bulk compositions varying from silicic alkaline or calc-alkaline to carbonatitic (e.g. see Table 7, Haggerty and Mariano, 1983). In general, the synthetic chevkinite/perrierite compositions obtained in these high-pressure experiments are higher in *REE* and alumina, and lower in iron (expressed

as FeO) than natural chevkinite/perrierite (e.g. McDowell, 1979; Ewart, 1981).

In view of the documented strontio-chevkinite compositions (with up to 20 wt. % SrO) (Haggerty and Mariano, 1983), the low $D_{Sr}^{chev/liq}$ values obtained in this work require comment. The ready accommodation of Sr in the chevkinite from the carbonatite may be linked directly to the associated high Zr and relatively low REE content, causing modification of the A sites, such that Sr substitutes into the lattice, at the expense of Ca and REE. Conversely, Sr may be discriminated against in the chevkinite lattice when there is a high total REE content and low Zr content, as in the compositions obtained in this work. These compositions show no negative correlation between REE and Sr contents, or positive correlation between Sr and Zr contents. However, the total variation in Sr and Zr is small (e.g. see examples in Table 2) so that these results do not necessarily preclude the earlier suggestion concerning Sr accommodation in chevkinite.

Chevkinite/perrierite crystallization from common magmas. Key essential structural constituents of chevkinite/perrierite are Ti and the REE, and saturation of a magma in these elements would be expected before chevkinite/perrierite crystallized. Ti-rich phase solubility (including chevkinite/perrierite) has been examined with respect to common magma compositions (Green and Pearson, 1986a), and it was shown that Ti-rich phase solubility decreases with increasing SiO₂ of the magma, and with decreasing *T*. A similar relationship appears to hold for the REE (e.g. compare ΣREE and SiO₂ contents of glasses formed at variable *T* coexisting with chevkinite/perrierite given in data in Figs. 4–7; e.g. for SiO₂ 67–68 wt. %, ΣREE of glass decreases from 1.4 wt. % to 0.8 wt. % as *T* changes from 1000 to 900 °C). Thus crystallization of chevkinite/perrierite is most likely from relatively evolved, SiO₂-rich magma at low *T*, and where the TiO₂ content has not been critically lowered by earlier precipitation of a Ti-rich phase, and where REE activity has increased because of earlier crystallization of phases with low D_{REE} . In magmas with high Ca and REE activity and low Ti activity, allanite may be expected instead of chevkinite/perrierite, or alternatively apatite and/or monazite may crystallize, if P-rich phase saturation is also achieved.

Conclusions

Experimental study of chevkinite/perrierite crystallization from common magmas enriched in Ti and REE components indicates that, given appropriate compositions, there is no *P* or *T* limit on chevkinite/perrierite stability, at least up to 20 kbar

and 1050 °C (Fig. 1). Thus if magmas become sufficiently enriched in Ti and REE, their subsequent evolution may involve crystallization of chevkinite/perrierite. Since Ti-rich phase saturation is almost inevitable in evolved, silica-rich magmas (Green and Pearson, 1986a), enrichment in REE becomes the key compositional parameter. Once chevkinite/perrierite saturation occurs, its fractionation from the host magma will have an important effect on lowering the REE content of further evolved compositions. This results from the ready partitioning of all the REE into chevkinite/perrierite, but in particular relative LREE depletion will occur, since the *D* values for the LREE are about an order of magnitude greater than for the HREE. Thus magmas which are derived from fractionation involving chevkinite/perrierite will show an increase in the HREE/LREE ratio. Such compositions have been documented (Miller and Mittlefehldt, 1982) and were attributed to allanite and/or monazite involvement. Separation of the relative importance of allanite, monazite or chevkinite/perrierite is difficult, since they all have similar LREE-enriched patterns (Miller and Mittlefehldt, 1982; this work).

Because of its demonstrated wide *P, T* stability, chevkinite/perrierite may also remain as a refractory, residual phase from the earliest stages of partial melting of deep crustal rocks, and in this context its recognition in granulite facies rocks is significant (De Paolo *et al.*, 1982).

Acknowledgements

This work has been funded by grants from the Australian Research Grants Scheme (E79/15170) and Macquarie University. Dr R. A. Day kindly read the manuscript and contributed constructive comment.

References

- De Paolo, D. J., Manton, W. I., Grew, E. S., and Halpern, M. (1982) *Nature* **298**, 614–18.
- Drake, M. J., and Weill, D. F. (1972) *Chem. Geol.* **10**, 179–81.
- Ewart, A. (1981) *J. Geophys. Res.* **86**, 10242–56.
- (1982) *J. Petrol.* **23**, 344–82.
- Exley, R. A. (1980) *Earth Planet. Sci. Lett.* **48**, 97–110.
- Gill, J. B. (1970) *Contrib. Mineral. Petrol.* **27**, 179–203.
- Green, T. H., and Pearson, N. J. (1985) *Ibid.* **91**, 24–36.
- (1986a) *Chem. Geol.* **55**, 185–201.
- (1986b) *Ibid.* **56**, 105–19.
- Ringwood, A. E., and Major, A. (1966) *J. Geophys. Res.* **71**, 3589–94.
- Haggerty, S. E., and Mariano, A. N. (1983) *Contrib. Mineral. Petrol.* **84**, 365–81.
- Hanson, G. N., and Langmuir, C. H. (1978) *Geochim. Cosmochim. Acta*, **42**, 725–41.

- Harding, A. R., Merriman, R. J., and Nancarrow, P. H. A. (1982) *Mineral. Mag.* **46**, 449-52.
- Izett, G. A., and Wilcox, R. E. (1968) *Am. Mineral.* **53**, 1558-67.
- Jaffe, H. W., Evans, H. T. Jr., and Chapman, R. W. (1956) *Ibid.* **41**, 474-87.
- McDowell, S. D. (1979) *Ibid.* **64**, 721-7.
- Miller, C. F., and Mittlefehldt, D. W. (1982) *Geol.* **10**, 129-33.
- Segalstad, T. V., and Larsen, A. O. (1978) *Am. Mineral.* **63**, 499-505.
- Shannon, R. D., and Prewitt, C. T. (1969) *Acta Crystallogr.* **25**, 925-46.
- Sun, S.-S., and Hanson, G. N. (1975) *Contrib. Mineral. Petrol.* **52**, 77-106.
- van Bergen, M. J. (1984) *Mineral. Mag.* **48**, 553-6.
- Watson, E. B., and Green, T. H. (1981) *Earth Planet. Sci. Lett.* **56**, 405-21.

[Manuscript received 18 November 1986;
revised 26 March 1987]